Nonlinear structures and thermodynamic instabilities in a one-dimensional lattice system

Nikos Theodorakopoulos[1,2], Michel Peyrard[3] and Robert S. MacKay[4]

[1] *Theoretical and Physical Chemistry Institute, National Hellenic Research Foundation, Vasileos Constantinou 48, 116 35 Athens, Greece*

[2] *Fachbereich Physik, Universität Konstanz, 78457 Konstanz, Germany*

[3] *Laboratoire de Physique, UMR-CNRS 5672, ENS Lyon, 46 Allée d'Italie, 69007 Lyon, France*

[4] *Mathematics Institute, University of Warwick, Coventry CV4 7AL, U.K.*

(Dated: September 20, 2004)

The equilibrium states of the discrete Peyrard-Bishop Hamiltonian with one end fixed are computed exactly from the two-dimensional nonlinear Morse map. These exact nonlinear structures are interpreted as domain walls (DW), interpolating between bound and unbound segments of the chain. The free energy of the DWs is calculated to leading order beyond the Gaussian approximation. Thermodynamic instabilities (e.g. DNA unzipping and/or thermal denaturation) can be understood in terms of DW formation.

PACS numbers: 87.10.+e, 63.70.+h, 05.70.Jk, 05.45-a

Computational results [1] have suggested, at varying levels of numerical rigor, that a class of one-dimensional lattice models proposed within a variety of physical contexts (e.g. interfacial wetting [2] or DNA denaturation [3]) may exhibit thermodynamic instabilities [4] which share many of the properties of ordinary phase transitions.

Owing to the lack of analytical results, it is important to explore alternative strategies which reveal exact features of these instabilities. One such strategy, which will be pursued in this work, is to exploit some of the tools of nonlinear dynamics in order to study the properties of the underlying exact equilibrium structures.

The general class of models under consideration is described by a Hamiltonian with a configurational part

$$H = \sum_{n=0}^{N} \left[\frac{1}{2R}(y_{n+1} - y_n)^2 + V(y_n) \right] \qquad (1)$$

where y_n is the displacement of the nth site, R is a dimensionless coupling constant and $V(y)$ is any potential with a repulsive core, a stable minimum and a flat top. We will deal with the case of a Morse potential [3], $V(y) = (1 - e^{-y})^2$.

We will demonstrate the existence of exact nonlinear structures which correspond to domain walls (DW)s, "interpolations" from the bound to the unbound phase. It will further be shown that the detailed stability properties of the DWs essentially determine the system's behavior with respect to both mechanical and thermal instabilities (unzipping and thermal melting, respectively, in the DNA context). Finally, we will use thermodynamic perturbation theory to account for the minor discrepancies which occur between the predictions of Gaussian DW-based theory and standard numerical results based on the transfer integral (TI) method. This work describes the case $R \gg 1$ (extreme discretization); DWs in the case $R \ll 1$ (continuum limit) have been treated in Ref. [5]. Unless otherwise stated, the value $R = 10.1$ will be used in numerical applications.

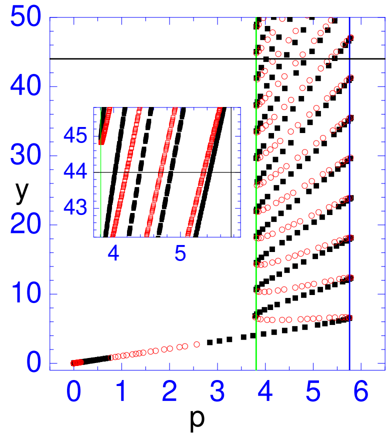

FIG. 1: The unstable manifold of the FP of the map (2) for $R = 10.1$ and $N = 28$. Black squares belong to stable equilibria, red open circles belong to unstable equilibria. The horizontal line at $y = 44$ demostrates the multivaluedness of the manifold as a function of y (4 stable and 3 unstable equilibria with that value of y; details in the inset). The vertical lines are drawn at p_{min} and p_{max}, the minimal and maximal asymptotic slopes of DWs.

The equilibria $\{y_n^{(\alpha)}\}$ of (1) are given by the two-dimensional map

$$\begin{aligned} p_{n+1}^{(\alpha)} &= p_n^{(\alpha)} + RV'(y_n^{(\alpha)}) \\ y_{n+1}^{(\alpha)} &= y_n^{(\alpha)} + p_{n+1}^{(\alpha)} \quad ; n = 0, 1, \cdots, N \end{aligned} \qquad (2)$$

which has a single hyperbolic fixed point (FP) at ($p^{(0)} = y^{(0)} = 0$). Equilibria can be classified as stable or unstable, according to whether all eigenvalues of the Hessian

$$A_{mn}^{(\alpha)} = \left. \frac{\partial^2 H}{\partial y_n \partial y_m} \right|_{\{y_i = y_i^{(\alpha)}\}} \qquad (3)$$

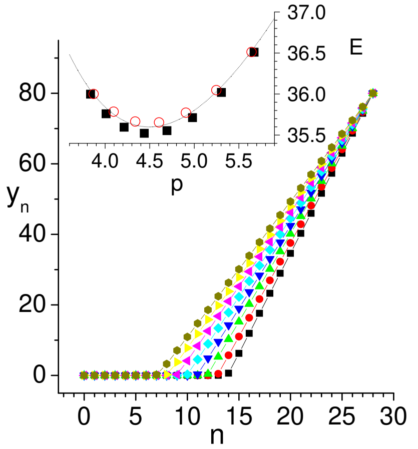

FIG. 2: The 8 stable equilibria corresponding to $N = 28$, $y_0 = 0$, $y_{N+1} = L = 80$. Not shown are 7 unstable equilibria enmeshed between the stable ones. Inset: total energies for both stable (black squares) and unstable (red open circles) equilibria. The continuous curve corresponds to a theoretical estimate which does not distinguish between stable and unstable equilibria (cf. text). Note that the typical energy difference - which does not shrink with increasing L - between neighboring extrema is about 0.15;

are nonnegative or not.

The tangent map at the FP is given by

$$\begin{pmatrix} \delta p \\ \delta y \end{pmatrix}_{n+1} = \begin{pmatrix} 1 & 2R \\ 1 & 1+2R \end{pmatrix} \begin{pmatrix} \delta p \\ \delta y \end{pmatrix}_{n} ; \qquad (4)$$

its eigenvalues are $\lambda_{\pm} = 1 + R \pm \sqrt{R^2 + 2R}$ and its corresponding (unnormalized) eigenvectors $\vec{\kappa}^{(\pm)} = (2R, R \pm \sqrt{R^2 + 2R})$, where the upper (lower) sign corresponds to the unstable (stable) manifold.

The structure of the unstable manifold of the FP is shown in Fig. 1. Its multivaluedness as a function of y turns out to have important consequences when the fixed-ends boundary conditions appropriate to the problem are introduced. These are of two types: (a) $y_0 = y_{N+1} = 0$, and (b) $y_0 = 0, y_{N+1} = L$. The only equilibrium compatible with (a) is the FP. In order to construct the equilibria compatible with (b), we generated a large number of sequences using the initial conditions $y_0 = 0$ and $p_0 = \kappa_2^+/\kappa_1^+ \exp(-s)$ with s uniformly spaced in an interval (s_1, s_2) and initially accepted a sequence if $|y_{N+1} - L|/L < 2 \cdot 10^{-5}$; a further scan of accepted sequences was made to eliminate sequences which are "immediate neighbors" in the manifold. The result for $L = 80$ is a total of 8 stable and 7 unstable such sequences. The stable ones are shown in Fig. 2; at the left they more or less coincide with the fixed point $y^{(0)} = 0$; to the right, they emerge as a bundle with linearly growing displacements and a range of slopes $p_{min} \leq p_\alpha \leq p_{max}$. The corresponding energies, according to (1) are shown in the inset as functions of the final slope p. Note that the unstable equilibria lie slightly above the neighboring stable ones. The overall dependence of the energy on the slope p can be understood by the following simple argument: each unbound site contributes an amount $1+p^2/(2R)$ to the energy; for $L \gg 1$, the number of unbound sites is approximately equal to L/p; hence $E(p, L) = (1/p + p/2R)L$; this is the dotted curve shown in the inset of Fig. 2. It follows that the minimum energy occurs at $p = p^* = (2R)^{1/2}$ and has value $E^*(L) = 2L/p^*$.

A few remarks are in order here: (i) The number of extrema grows linearly with L; more precisely, for sufficiently large L, the number of local minima is $[L/p_{min}] - [L/p_{max}] + 1$; locally unstable extrema are fewer by one. (ii) There are no zero eigenvalues for any extrema, except for discrete L at which a new pair is created. (iii) The unstable extrema (minmax) have only one negative eigenvalue; the rest of their spectrum is essentially identical with that of neighboring local minima. (iv) For large R, the limits p_{min}, p_{max} are asymptotically $p_{min} \sim \ln(2R) + 1$, $p_{max} \sim R/2 + \ln 2$, which we derived by approximate solution of the equations for the unstable manifold. (v) The energy spacing (Peierls barrier) between the absolute minimum and the minmax with the lowest energy (cf. inset in Fig. 2) is about 0.15. (vi) For any given equilibrium (DW) with a transverse displacement $L \gg 1$ and final slope p, the quantity $dE/dL = V'(L) + (L - y_N)/R \approx p/R$ represents the force acting on the end particle. In the case of the absolute minimum, $p = p^*$, this is equal to $f_0 = (2/R)^{1/2}$; in the context of DNA denaturation models, it corresponds to the force required to bring about mechanical "unzipping" at zero temperature.

What happens at nonzero temperatures? In order to examine the relevance of DWs for thermodynamics, it is necessary to look at the partition functions $Z_N(0)$ and $Z_N(L)$ which correspond to the two types of boundary conditions (cf. above) respectively. We will consider $1 \ll L \ll N$; the difference in the free energies

$$\Delta G = -T \lim_{N \to \infty} \ln \left\{ \frac{Z_N(L)}{Z_N(0)} \right\} \qquad (5)$$

is the quantity of interest; in particular, the derivative $(\partial \Delta G/\partial L)_T$ is equal to the force $f(L, T)$ required to maintain the right end of the chain at a given tranverse displacement L. For small displacements around any equilibrium, $y_n = y_n^{(\alpha)} + \psi_n$, the Hamiltonian can be expanded as

$$H^{(\alpha)}(\{\psi\}) \approx E^{(\alpha)} + \frac{1}{2} \sum_{m,n} A_{mn}^{(\alpha)} \psi_m \psi_n + \sum_m v_{m,\alpha}^{(3)} \psi_m^3 + \sum_m v_{m,\alpha}^{(4)} \psi_m^4 , \qquad (6)$$

where $v_{m,\alpha}^{(j)} = V^{(j)}(y_m^{(\alpha)})/j!$, and terms of higher than

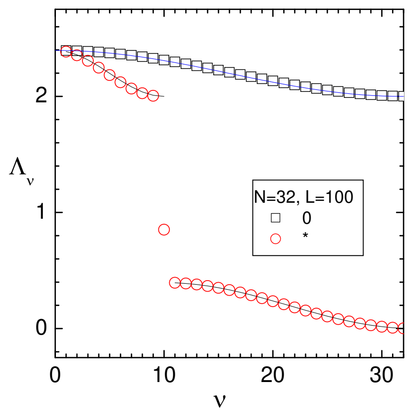

FIG. 3: Eigenvalue spectra of the hessians $A^{(0)}$ (open squares) and $A^{(*)}$ (open circles) for $N = 32$ and $L = 100$. The DW's spectrum consists of bands of optical and acoustic phonons, localized respectively in the bound and unbound portions of the chain, and a single local mode in the gap; both bands are well described (to order $\mathcal{O}(1/L)$) by the corresponding free phonon dispersion curves (dotted).

fourth order have been dropped. The partition function

$$Z_N^{(\alpha)} = \int_{-\infty}^{+\infty} \prod_{j=1}^{N} d\psi_j \; e^{-H^{(\alpha)}(\{\psi\})/T} \tag{7}$$

can be calculated in the Gaussian approximation by keeping terms up to second order in (6). The result is [6]

$$Z_N^{(\alpha)} \approx e^{-E^{(\alpha)}/T} \prod_\nu \left\{ 2\pi T/\Lambda_\nu^{(\alpha)} \right\}^{1/2} \quad , \tag{8}$$

where $\{\Lambda_\nu^{(\alpha)}\}$, $\nu = 1, 2, ..., N$ are the eigenvalues of the Hessian matrix $A^{(\alpha)}$.

Eq. (8) will be applied twice. First, to evaluate $Z_N(0)$; in this case, the relevant equilibrium is the FP. Second, to evaluate $Z_N(L)$, in which case the relevant equilibrium is the DW with the minimal energy and the final slope p^* (cf. above). Note that at temperatures of order 1 or higher (relevant for the occurrence of macroscopic instabilities), the roughness of the energy landscape (Fig. 2), typified by the height of the Peierls barrier (cf. comment (v) above), essentially disappears.

The ratio of partition functions in (5) can be approximated as

$$\frac{Z_N(L)}{Z_N(0)} \approx e^{-E^{(*)}/T} \prod_\nu \left\{ \Lambda_\nu^{(0)}/\Lambda_\nu^{(*)} \right\}^{1/2} \quad . \tag{9}$$

The eigenvalue spectra $\{\Lambda_\nu^{(*)}, \Lambda_\nu^{(0)}\}$ are shown in Fig. 3. As has already been pointed out in the context of the continuum-limit[5], the DW acts as an interface between bound and unbound phases; the unbound phase supports only acoustic phonons and the bound phase only optical ones. The quantity

$$\Omega = \frac{1}{2} \sum_{\nu=1}^{N} \ln \left\{ \Lambda_\nu^{(0)}/\Lambda_\nu^{(*)} \right\} = \frac{L}{p^*}\sigma + \mathcal{O}(1) \, , \tag{10}$$

where $\sigma = \ln\left(\sqrt{R/2} + \sqrt{1 + R/2}\right)$, is found to be, for $1 \ll L/p^* \ll N$, independent of N and proportional to the number L/p^* of unbound sites; the reason is that, as can be seen from Fig. 3, the optical phonons in the unbound region of the DW cover exactly the frequency range of the optical phonons around the fixed point, and therefore cancel out in taking the ratio; this leaves only a dependence on the ratio between acoustic and optical frequencies for a number of modes of order L/p^*. The proportionality constant $\sigma(R)$ has been calculated in Ref. [5] using the argument sketched above, without reference to the exact eigenvalue spectrum. Irrelevant corrections of order unity originate from the transition region of the DW and/or the single localized oscillation mode. Inserting (10) and (9) in (5), we obtain, in the Gaussian approximation,

$$\Delta G \approx E^*(L) - T\Omega = (2 - T\sigma)\,\frac{L}{p^*} \quad . \tag{11}$$

It follows that the force now required to maintain the chain at (any) transverse displacement $L \gg p^*$,

$$f(T) \approx \frac{1}{p^*}\,(2 - T\sigma) \quad , \tag{12}$$

is reduced as a result of thermal motion. At $T = 2/\sigma$ this generalized unzipping force vanishes; spontaneous formation of the DW becomes possible. In the context of DNA denaturation theory, this amounts to spontaneous melting (thermal denaturation). That transition has been extensively studied, assuming periodic boundary conditions, both in the continuum and the discrete regime by means of the TI method. The critical temperature $2/\sigma$ obtained in the Gaussian approximation is in good agreement with the TI results for values of $R \lesssim 4$; systematic deviations occur at higher R however[5].

It is possible to improve the calculation of ΔG by going beyond the Gaussian approximation. Standard thermodynamic perturbation theory[6] can be applied to evaluate the contribution of cubic and quartic terms in (6) to the partition function (7), - again, both for the FP and the DW - and to derive a low-temperature expansion for the resulting free energy. Each power of the displacement field in (6) contributes a factor $T^{1/2}$. The irreducible graphs which contribute to $\ln Z_N^{(\alpha)}$ to leading order in the temperature are:

$$= -3T \sum_m v_{m,\alpha}^{(4)} \{g_{mm}^\alpha\}^2 \quad \text{, and} \tag{13}$$

$$= 6T \cdot \frac{1}{2} \sum_m v_{m,\alpha}^{(3)} v_{n,\alpha}^{(3)} \{g_{mn}^\alpha\}^3 \quad , \tag{14}$$

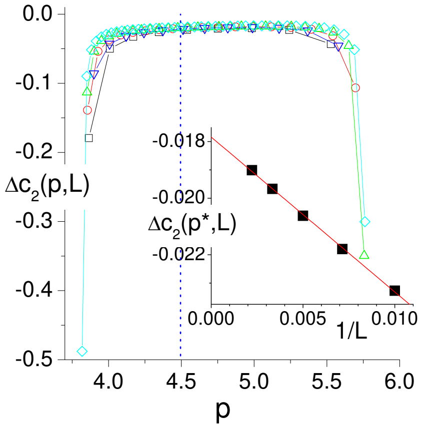

FIG. 4: Lowest order anharmonic correction to the free energy difference ΔG: The coefficient $\Delta c_2(p, L)$ for $L = 100, 140, 200, 300, 450$ vs. p; for each L the difference $(C_2(p) - C_2^0)/L$ is numerically evaluated at all stable minima; the interpolates taken at $p = p^*$ are plotted against $1/L$ (inset); this procedure extrapolates to a value $\Delta c_2^* = -0.01784(5)$.

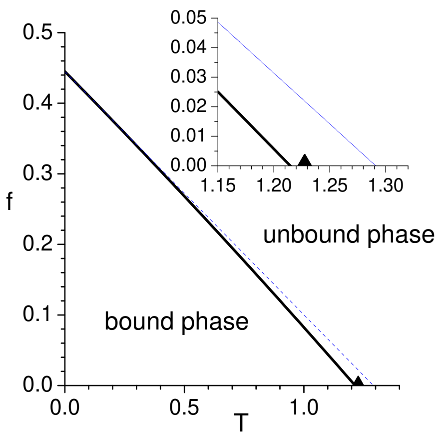

FIG. 5: Phase diagram in the $f - T$ plane. The dotted line is obtained on the basis of the Gaussian approximation (predicted $T_c = 1.291$). The solid line is Eq. 15 with $\Delta c_2^* = -0.01784$ (cf. Fig. 4). Inset: detail of critical region, showing a predicted $T_c = 1.215$; the triangle is the result of a finite-size scaling numerical TI calculation $T_c = 1.227$ [1c].

where $g_{mn}^{(\alpha)}$ is the relevant Green's function (inverse of the Hessian evaluated at the equilibrium α).

Let $-TC_2^\alpha$ denote the sum of the two contributions above. The correction to the free energy ΔG will be obtained as a difference between values at the two relevant equilibria (FP and DW with minimal energy); the quantity $C_2^{(*)} - C_2^{(0)}$ is expected to be independent of N and proportional to the length of the unbound segment (cf. above). Fig. 4 (inset) displays the values of $\Delta c_2(p^*) = (C_2^{(*)} - C_2^{(0)})/L$ (interpolated from the values at the closest DW's, displayed in the main figure) for a series of L-values. The extrapolated value $\Delta c_2^* = \lim_{L\to\infty} \Delta c_2(p^*, L)$ can be used as a correction to eqs. 11 and 12 above, i.e.

$$f(T) \approx \frac{1}{p^*}(2 - T\sigma) + \Delta c_2^* T^2 \quad . \tag{15}$$

The resulting phase diagram is shown in Fig. 5. The predicted $T_c = 1.215$ is in good agreement with the numerical TI calculation [1c] $T_c^{TI} = 1.227$.

We conclude with two remarks. The first is a caution about the inherent limitations of the low-order perturbational approach used. At lower values of R, which tend to increase T_c to values substantially higher than 1, it cannot be expected to work (although the Gaussian approximation produces very good estimates of T_c). At much higher values of R, the perturbation terms in the Hamiltonian become too large compared with the Gaussian approximation; again, one would presumably have to include higher order terms to obtain reasonable results.

The second remark concerns a further prospect: including nonlinear stacking terms in the Hamiltonian [7] has been known to produce real or apparent first order transitions. It would be interesting to explore how this behavior would be reflected in the DW approach.

Part of this work was performed while one of us (N.T.) was visiting Lyon and Warwick; he wishes to thank both departments for hospitality. Financial support from EU contract HPRN-CT-1999-00163 (LOCNET network) is acknowledged.

[1] (a) T. Dauxois and M. Peyrard, Phys. Rev. E **51**, 4027 (1995); (b) Y-L Zhang, W-M Zheng, J-X Liu, Y. Z. Chen, Phys. Rev. E **56**, 7100 (1997); (c) N. Theodorakopoulos, Phys. Rev. E **68**, 026109 (2003); (d) N. Theodorakopoulos, in *Localization and energy transfer in nonlinear systems*, L.Vazquez, R.S. MacKay and M.P. Zorzano (Eds.), pp. 130-152, World Scientific (2003); cond-mat/0210188 (review article).

[2] D. M. Kroll and R. Lipowski, Phys. Rev. B **28**, 5273 (1983); R. Lipowski, Phys. Rev. B **32**, 1731 (1985).

[3] M. Peyrard and A.R. Bishop, Phys. Rev. Lett. **62**, 2755 (1989).

[4] Thermal DNA denaturation is reviewed by R.M. Wartell and A.S. Benight, *Physics Reports* **126**, 67 (1985). Mechanical separation of the two strands was first achieved by B. Essevaz-Roulet, U. Bockelmann and F. Heslot, *Proc.*

Nat. Acad. Sci. USA **94** 11935 (1997); cf. also recent experiments which have revealed interesting structural transitions under torque and tension on DNA (Z. Bryant, M.D. Stone, J. Gore, S.B. Smith, N.R. Cozzarelli, C. Bustamente, Nature **424**, 338 (2003)).

[5] T. Dauxois, N. Theodorakopoulos and M. Peyrard, J. Stat. Phys. **107**, 869 (2002).

[6] D.J. Amit, *Field theory, the renormalization group and critical phenomena*, Addison-Wesley, New York (1978).

[7] N. Theodorakopoulos, T. Dauxois and M. Peyrard, Phys. Rev. Lett. **85**, 6 (2000).